Robust Sliding Mode Control for Two-Wheel Robot Without Kinematic Equations

Arash Mousaei (a.mousaei1994@gmail.com)
University of Tabriz
Meysam Gheisarnejad (m.gheisar@ece.au.dk)
University of Aarhus
Mohammad Hasan Khooban (khooban@ece.au.dk)
University of Aarhus

Research Article

Keywords: Two-Wheel Robot, Sliding Mode Control, Uncertainties, Kinematic Equations

DOI: https://doi.org/10.21203/rs.3.rs-2652334/v1

Robust Sliding Mode Control for Two-Wheel Robot Without Kinematic Equations

A. Mousaei[1], M. Gheisarnejad[2], and M. H. Khooban[3]

[1]Department of Electrical Engineering University of Tabriz, Tabriz, Iran

[2,3]Department of Electrical and Computer Engineering, Aarhus University, 8200 Aarhus, Denmark

Abstract. This article proposes solutions to control the balance of a two-wheel robotic system in the presence of uncertainties in the dynamic equations and without the need for kinematic equations. To do this, the dynamic equations of this system are first transferred to the error area and then these equations are divided into two completely independent subsystems, under excitation, and full excitation. In the following, two completely different sliding mode controllers are presented to control the under-excitation subsystem, which can make this subsystem asymptotically stable in the presence of structural and non-structural uncertainties. After that, a sliding mode control is proposed to control the entire excitation subsystem, making this subsystem asymptotically stable in the presence of existing uncertainties. Since these two subsystems are completely independent of each other, proving their global asymptotic stability provides proof of the global asymptotic stability of the closed-loop system. The isolation of two-wheel balancing robot subsystems eliminates the need to use kinematic equations, resulting in structural uncertainties not affecting the tracking accuracy of closed-loop system state variables. Finally, to verify the performance of the proposed controllers and compare their performance results, three-stage simulations are implemented on the two-wheel Balance robotic system. Mathematical proofs and simulation results show the optimal performance of the proposed solutions.

Keywords: *Two-Wheel Robot, Sliding Mode Control, Uncertainties, Kinematic Equations.*

1. Introduction

In the contemporary era, robotics is one of the advanced fields of technology and engineering sciences that has found a special place in human life. In the meantime, the balance two-wheel robot system with non-holonomic constraints has many applications in different fields [1]. The balance two-wheel robot system is placed in the category of mobile robots and its design is somehow inspired by the inverted pendulum system. Low weight, small wheels, high rotation speed, and overall high maneuverability are

the main features of this system. These features have caused it to have many uses in factories as a personnel and equipment carrier or even as a fun device for children in parks. It should be noted that there is no need to use fossil fuels to move the two-wheel balance robot and it does not make any noise during movement.

The balanced two-wheel robot system has two wheels connected, the body of the system is mounted on this axis, and the wheels are driven by DC motors. Therefore, this system with this mechanical structure is inherently unstable and has highly non-linear dynamics [2] and [3]. Based on this, the first goal of the controller should be to maintain balance and prevent this system from being overthrown, and its secondary goal is to guide the system on the desired path [4].

1. 1. Review of the previous articles

Before now, many researchers like M. Baloh et.al [5], A. Salerno et.al [6], and Y. Kim et.al [7] studied the modeling and control of the balanced two-wheel robot system. D. Takei et.al [8], and W. Junfeng et.al used the feedback controller to control of the two-wheel robot. According to the results of experiments of [8] and [9], there is a big difference between the real model and the linearized model of the system, therefore, in case of external disturbances, the instability of the two-wheel robot system is inevitable. K. Pathak et.al [10] proposed a non-linear controller to stabilize and control the balanced two-wheel robot system. In the proposed control design, it is assumed that an accurate model of this system is available and the controller is not exposed to any uncertainty. Therefore, in case of uncertainty and external disturbances, the balance of the robot will be disturbed and the system will become unstable. To deal with existing uncertainties, C. H. Chiu [11], proposed an adaptive output recurrent cerebellar model controller, H. T. Yau et.al [12] propounded a robust control, S. C. Lin et.al [13] suggested a nonlinear adaptive sliding mode control, J. Wu et.al [14] presented a solution to control the two-wheel robot system using robust and adaptive control methods, and A. Wasif [15] et.al introduced a two-level adaptive control. Although the proposed solutions are successful in overcoming the existing uncertainties, their design steps are very complex and have a very high number of calculations.

In the last two decades, intelligent controllers such as fuzzy control and neuronal network have been used to control the balance two-wheel robot system. R. D. Pinzon-Morales and Y. Hirata [16] proposed a neuronal network model for adaptive robot control. K. H. Su and Y. Y. Chen [17] controlled a two-wheel robot via a neural-fuzzy technique. J. Wu and S. Jia [18] presented a T-S adaptive neural network fuzzy control. C. H. Chiu et.al [19] propounded a real-time control of a wheeled inverted pendulum based on an intelligent model-free controller. W. Zeng et.al [20] learned a 2-wheel robot using an adaptive neural network controller. Y. Dai et.al [21] proposed a control method based on the fuzzy sliding mode controller. To design the proposed controllers, engineers must conduct very detailed studies in the field of the mechanical structure of the two-wheel robot system, so that based on that they can determine the membership functions in the rule base of this type of controller. On the other hand, to maintain the balance of the two-wheel robot system and create the controller tracking conditions, the designers should use the multi-input-multiple-output fuzzy rules in the fuzzy rules database of the

inference engine related to this type of controllers, and increase the tracking accuracy, the number of these fuzzy rules should also be increased. This greatly increases the volume of the controller's input calculations, and if there is a delay in the controller's input calculations, it becomes impossible to guarantee the stability of the system. In [22], a learning algorithm, which is considered one of the smart methods, has been used to control the two-wheel balance robot system by M. H. Khooban et.al. Since in this algorithm, the learning time calculations are done online, so the computational volume of the proposed solution is also very large and it is difficult to adjust and use it in an inherently unstable system such as a balanced two-wheel robot system.

So far, sliding mode control has been very successful in controlling robotic systems [23] to [32]. This control method has advantages such as insensitivity to changes in system parameters, robustness to external disturbances, quick response, and easy implementation. J. Huang et.al [23], used a sliding mode controller to control a special form of the balanced two-wheel robot system. H. T. Yau et.al [24], N. M. A. Ghani et.al [25], and J. Wu et.al [26] used only this control method to maintain the balance of the two-wheel robot and did not propose a solution to track the desired path. Mathematical proof and simulation results show the performance of the proposed controllers, but the problem of maintaining balance limits the application of the balanced two-wheel robot in real-time. S. C. Lin et.al [27] introduced the balanced two-wheel robot as a vehicle and used the adaptive sliding mode control method to maintain balance and control its angle around the transverse axis in the presence of uncertainties. F. Dai et.al [28] proposed a solution for maintaining balance and accurate tracking control of a balanced two-wheel robot with a small center of mass using sliding mode control. A. Filipescu et.al [29] introduced a discrete-time sliding mode controller to track the optimal path of a balanced two-wheel robot. M. Yue, et.al [30], M. Cui et.al [31], and W. Wang et.al [32] used sliding mode control and adaptive sliding mode control to control the tracking of the balanced two-wheel robot system in the presence of structural uncertainties.

Although the effect of structural and non-structural uncertainties in the dynamic equations has been taken into account in the design of the mentioned solutions, in all that, the kinematic equations of this system have been used to maintain the balance of the two-wheel robot and control its accurate tracking. Therefore, in case of uncertainties, the kinematic equations of the balanced two-wheel robot system are changed. Since in the proposed methods, only the role of the presence of structural and non-structural uncertainties in the dynamic equations has been considered and, in all designs, the assumption of certainty in the kinematic equations is established, therefore the proposed controllers are not able to overcome the uncertainties in the kinematic equations and this exposes the stability of the system to instability and greatly increases the tracking error.

1. 2. Contributions

The main contributions of this work are summarized below:

I. In this article, using the sliding mode control method to maintain the balance of the balanced two-wheel robot system and its precise tracking control, controllers are proposed that can overcome the uncertainties in the dynamic equations of the two-wheel robot. Since there is no need to use the kinematic equations of the two-wheeled robot in the design and implementation of the proposed solution, therefore, the occurrence of uncertainty in these equations cannot affect the performance of the proposed controllers and the stability of the system.

II. In the mentioned articles in the previous section, researchers have controlled the balanced two-wheel robot system using two types of controllers. One of the controllers is placed in the outer loop and the other one is designed to control the inner loop. Kinematic control of the robot system is done through the outer loop controller and dynamic control is done through the inner controller. In this article, solutions are proposed that perform kinematic control and dynamic control of the balance two-wheeled robot system through a controller. In this case, both the number of controllers and the economic cost of practical implementation of the controller will be reduced.

III. Because in the proposed controller design method, the dynamic equations of the balance two-wheeled robot system are divided into two sub-systems of full-excitation and under-excitation, and the design of the proposed controllers is done step by step, this makes learning the controller design process simple for students and control engineers. Because the separation of the subsystems is done completely, the effect of each of these subsystems on the performance of the controllers is evident, and this makes it easier to adjust the input coefficients of the controllers.

IV. In the design of the proposed controllers, the conditions of their practical implementation in terms of the number of the coefficients of the control's input, the volume of calculations, and the maximum range of the control input have been taken into account so that the proposed solutions can be implemented in practice.

In the following, the structure of the article is presented in part 2 of the modeling of the balanced two-wheel robot system. In section 3, the dynamic equations of the robot are transferred to the field of state equations, and then in section 4, they are transferred to the error field and divided into two sub-systems: under-excitation and full-excitation. Section 5 is dedicated to the design of the first proposed sliding mode control for sub-excitation and all-excitation subsystems, and in this section, the stability of the system in the presence of the proposed controllers is presented. In section 6, the design of the second proposed sliding mode control for the sub-excitation subsystem and the proof of the stability of the closed-loop system are described. Section 7 examines the benefits and comparison of the proposed sliding mode controllers for the sub-propulsion subsystem, and then in Section 8, simulations are

implemented in 3 stages on the balanced two-wheeled robot system to examine the performance of the proposed controllers. Finally, section 9 is devoted to conclusions.

2. Modeling of the balanced two-wheel robot system

In the two-wheel robot system, there is no slippage between the wheel and the ground. Figure 1 shows the balanced two-wheel robot system, and Kane's method was used to develop the system model [33-34]. In this system, F is the Newtonian force, S is the body of the robot, C_1 is the left wheel, and C_2 is the right wheel of the system. Also, n_1, n_2, and n_3 are defined by the unit vectors on the center of the connecting rod between the two wheels. Table 1 shows some important mechanical parameters of the system. Finally, using the Euler-Lagrange method, the final dynamic equations of the system are obtained as follows [34].

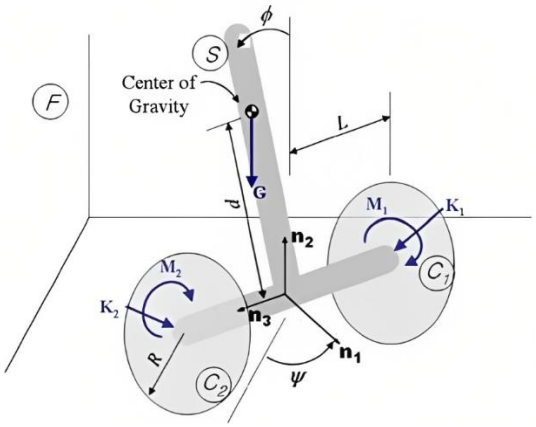

Fig 1. Balanced two-wheel robot system assuming applied forces.

$$3(m_c + m_s)\ddot{x} - m_s d\cos(\emptyset)\ddot{\emptyset} + m_s d\sin(\emptyset)\left(\dot{\emptyset}^2 + \dot{\psi}^2\right) = -\frac{\tau_1 + \tau_2}{R} \tag{1}$$

$$\left[3\left(L^2 + \frac{1}{2R^2}\right)m_c + m_s d^2 sin^2(\emptyset) + I_2\right]\ddot{\psi} + m_s d^2 \sin(\emptyset)\cos(\emptyset)\,\dot{\psi}\dot{\emptyset} = \frac{L}{R}(\tau_1 - \tau_2) \tag{2}$$

$$m_s d\cos(\emptyset)\ddot{x} - (m_s d^2 - I_2)\ddot{\emptyset} + m_s d^2 \sin(\emptyset)\cos(\emptyset)\,\dot{\emptyset}^2 + m_s g d\sin(\emptyset) = \tau_1 + \tau_2 \tag{3}$$

Table 1. Important mechanical parameters of the balanced two-wheeled robot system

Mechanical Parameter	Description	Amount	Value
d	The distance between C and C.G	0.1	m
m_s	Body mass	4.315	Kg
I_2	The direct rotational inertia of the body along the axis perpendicular to the axis between the two wheels	3.679e-3	$Kg.m^2$
I_3	The direct rotational inertia of the body along the axis of the axle between the two wheels	28.07e-3	$Kg.m^2$
L	Half the distance between the two wheels	0.1	m
R	Radius of each wheel	0.073	m
m_c	Mass of each wheel	0.503	Kg

- *Transferring the dynamic equations to the state space domain*

In this section, the dynamic equations of the balanced two-wheel robot are transferred to the domain of the state space. For this purpose, the equation of (3) is arranged as follows, and we will have:

$$\ddot{x} = \frac{1}{m_s d\cos(\emptyset)}\left[(m_s d^2 + I_2)\ddot{\emptyset} - m_s d^2 \sin(\emptyset)\cos(\emptyset)\,\dot{\emptyset}^2 - m_s g d\sin(\emptyset) + \tau_1 + \tau_2\right] \tag{4}$$

Then, by replacing equation (4) in (1), we have:

$$\frac{3(m_c + m_s)}{m_s d\cos(\emptyset)}\left[(m_s d^2 + I_2)\ddot{\emptyset} - m_s d^2 \sin(\emptyset)\cos(\emptyset)\,\dot{\emptyset}^2 - m_s g d\sin(\emptyset) + \tau_1 + \tau_2\right] \tag{5}$$

$$- m_s d\cos(\emptyset)\ddot{\emptyset} + m_s d\sin(\emptyset)\left(\dot{\emptyset}^2 + \dot{\psi}^2\right) = -\frac{\tau_1 + \tau_2}{R}$$

In the following:

$$\left[\frac{3(m_c + m_s)(m_s d^2 + I_2)}{m_s d\cos(\emptyset)} m_s d\cos(\emptyset)\right]\ddot{\emptyset} = \tag{6}$$

$$\frac{3(m_c + m_s)}{m_s d\cos(\emptyset)}\left[m_s d^2 \sin(\emptyset)\cos(\emptyset)\,\dot{\emptyset}^2 + m_s g d\sin(\emptyset)\right]$$

$$-\frac{3(m_c + m_s)}{m_s d\cos(\emptyset)}(\tau_1 + \tau_2) - \frac{\tau_1 + \tau_2}{R}$$

And:

$$\left[\frac{3(m_c + m_s)(m_s d^2 + I_2)}{m_s d\cos(\emptyset)} m_s d\cos(\emptyset)\right]\ddot{\emptyset} = \tag{7}$$

$$\frac{3(m_c + m_s)}{m_s d\cos(\emptyset)}\left[m_s d^2 \sin(\emptyset)\cos(\emptyset)\,\dot{\emptyset}^2 + m_s g d\sin(\emptyset)\right]$$

$$-\left[\frac{3(m_c + m_s)}{m_s d\cos(\emptyset)} - \frac{1}{R}\right](\tau_1 + \tau_2)$$

By rewriting relation (7), we will have:

$$\ddot{\emptyset} = \frac{3(m_c + m_s)}{3(m_c + m_s)(m_s d^2 + I_2) - (m_s d\cos(\emptyset)^2)} \times \left[m_s d^2 \sin(\emptyset)\cos(\emptyset)\,\dot{\emptyset}^2 + m_s g d\sin(\emptyset)\right] \tag{8}$$

$$-\left[\frac{m_s d\cos(\emptyset)}{3(m_c + m_s)(m_s d^2 + I_2) - (m_s d\cos(\emptyset)^2)}\right] \times$$

$$\left[\frac{3R(m_c + m_s) + m_s d\cos(\emptyset)}{R m_s d\cos(\emptyset)}\right](\tau_1 + \tau_2)$$

To express the state equations of the system, the following variables are introduced:

$$\emptyset = x_1 \quad , \quad \dot{\emptyset} = x_2 \quad , \quad x = x_3 \tag{9}$$

$$\dot{x} = x_4 \quad , \quad \dot{\psi} = x_5 \quad , \quad \dot{\psi} = x_6$$

According to this state variables, the following nonlinear functions are defined:

$$f_1(x_1, x_2) = \frac{3(m_c + m_s)}{3(m_c + m_s)(m_s d^2 + I_2) - (m_s d\cos(\emptyset)^2)} \tag{10}$$

$$\times \left[m_s d^2 \sin(\emptyset)\cos(\emptyset)\,\dot{\emptyset}^2 + m_s g d\sin(\emptyset)\right]$$

$$g_1(x_1) = -\left[\frac{m_s d\cos(\emptyset)}{3(m_c + m_s)(m_s d^2 + I_2) - (m_s d\cos(\emptyset)^2)}\right] \times \left[\frac{3R(m_c + m_s) + m_s d\cos(\emptyset)}{R m_s d\cos(\emptyset)}\right](\tau_1 + \tau_2) \quad (11)$$

By inserting (11) and (10) in relation (8), we will have:

$$\ddot{\emptyset} = f_1(x_1, x_2) + g_1(x_1)(\tau_1 + \tau_2) \quad (12)$$

In the following, the relation (8) is placed in (4):

$$\ddot{x} = \frac{(m_s d^2 + I_2)}{m_s d\cos(\emptyset)}\ddot{\emptyset} + \frac{1}{m_s d\cos(\emptyset)}\left[m_s d^2 \sin(\emptyset)\cos(\emptyset)\,\dot{\emptyset}^2 + m_s g d\sin(\emptyset)\right] + \frac{1}{m_s d\cos(\emptyset)}(\tau_1 + \tau_2) \quad (13)$$

$$\ddot{x} = \frac{(m_s d^2 + I_2)}{m_s d\cos(\emptyset)} \times \frac{3(m_c + m_s)}{3(m_c + m_s)(m_s d^2 + I_2) - (m_s d\cos(\emptyset)^2)} \times \left[m_s d^2 \sin(\emptyset)\cos(\emptyset)\,\dot{\emptyset}^2 + m_s g d\sin(\emptyset)\right] - \frac{(m_s d^2 + I_2)}{m_s d\cos(\emptyset)}\left[\frac{m_s d\cos(\emptyset)}{3(m_c + m_s)(m_s d^2 + I_2) - (m_s d\cos(\emptyset)^2)}\right] \times \left[\frac{3R(m_c + m_s) + m_s d\cos(\emptyset)}{R m_s d\cos(\emptyset)}\right](\tau_1 + \tau_2) + \frac{1}{m_s d\cos(\emptyset)}\left[m_s d^2 \sin(\emptyset)\cos(\emptyset)\,\dot{\emptyset}^2 + m_s g d\sin(\emptyset)\right] + \frac{1}{m_s d\cos(\emptyset)}(\tau_1 + \tau_2) \quad (14)$$

The above equation is simplified as (15) and based on the defined state variables, non-linear functions (16) and (17) are introduced. Equations (17) and (16) are placed in (15):

$$\ddot{x} = \left[m_s d^2 \sin(\emptyset)\cos(\emptyset)\,\dot{\emptyset}^2 + m_s g d\sin(\emptyset)\right]\left[\frac{(m_s d^2 + I_2)}{m_s d\cos(\emptyset)} \times \frac{3(m_c + m_s)}{3(m_c + m_s)(m_s d^2 + I_2) - (m_s d\cos(\emptyset)^2)} - \frac{1}{m_s d\cos(\emptyset)}\right] + \left[\frac{1}{m_s d\cos(\emptyset)} - \frac{(m_s d^2 + I_2)}{3(m_c + m_s)(m_s d^2 + I_2) - (m_s d\cos(\emptyset)^2)} \times \frac{3R(m_c + m_s) + m_s d\cos(\emptyset)}{R m_s d\cos(\emptyset)}\right](\tau_1 + \tau_2) \quad (15)$$

$$f_2(x_1, x_2) = \left[m_s d^2 \sin(\emptyset)\cos(\emptyset)\,\dot{\emptyset}^2 + m_s g d\sin(\emptyset)\right]\left[\frac{(m_s d^2 + I_2)}{m_s d\cos(\emptyset)} \times \frac{3(m_c + m_s)}{3(m_c + m_s)(m_s d^2 + I_2) - (m_s d\cos(\emptyset)^2)} - \frac{1}{m_s d\cos(\emptyset)}\right] \quad (16)$$

$$g_2(x_1) = \left[\frac{1}{m_s d\cos(\emptyset)} - \frac{(m_s d^2 + I_2)}{3(m_c + m_s)(m_s d^2 + I_2) - (m_s d\cos(\emptyset)^2)} \times \frac{3R(m_c + m_s) + m_s d\cos(\emptyset)}{R m_s d\cos(\emptyset)}\right](\tau_1 + \tau_2) \quad (17)$$

And we will have:

$$\ddot{x} = f_2(x_1, x_2) + g_2(x_1)(\tau_1 + \tau_2) \tag{18}$$

In the following, relation 2 is rewritten as follows:

$$\ddot{\psi} = -\frac{m_s d^2 \sin(\emptyset)\cos(\emptyset)\,\dot{\psi}\dot{\emptyset}}{\left[3\left(L^2 + \frac{1}{2R^2}\right)m_c + m_s d^2 sin^2(\emptyset) + I_2\right]} + \frac{L(\tau_1 - \tau_2)}{R\left[3\left(L^2 + \frac{1}{2R^2}\right)m_c + m_s d^2 sin^2(\emptyset) + I_2\right]} \tag{19}$$

Based on the stated state variables, the following nonlinear functions are introduced and then inserted into (19).

$$f_3(x_1, x_2, x_6) = -\frac{m_s d^2 \sin(\emptyset)\cos(\emptyset)\,\dot{\psi}\dot{\emptyset}}{\left[3\left(L^2 + \frac{1}{2R^2}\right)m_c + m_s d^2 sin^2(\emptyset) + I_2\right]} \tag{20}$$

$$g_3(x_1) = \frac{L}{R\left[3\left(L^2 + \frac{1}{2R^2}\right)m_c + m_s d^2 sin^2(\emptyset) + I_2\right]} \tag{21}$$

$$\ddot{\psi} = f_3(x_1, x_2, x_6) + g_3(x_1)(\tau_1 - \tau_2) \tag{22}$$

In the following, with the definition of $\tau_1 + \tau_2 = u_1$ and $\tau_1 - \tau_2 = u_2$, and based on the functions f_1, g_1, f_2, g_2, f_3, and g_3 in relations (8), (15), and (19) the dynamic equations of the balanced two-wheel robot in the domain of the state space will be as follows:

$$\begin{aligned} &\dot{x}_1 = x_2 \quad , \quad \dot{x}_2 = f_1(x_1, x_2) + g_1(x_1)u_1(t) + d_1(t) \\ &\dot{x}_3 = x_4 \quad , \quad \dot{x}_4 = f_2(x_1, x_2) + g_2(x_1)u_1(t) + d_2(t) \\ &\dot{x}_5 = x_6 \quad , \quad \dot{x}_6 = f_3(x_1, x_2, x_6) + g_3(x_1)u_2(t) + d_3(t) \end{aligned} \tag{23}$$

Which d_1, d_2, and d_3 represent unmodeled dynamics and external disturbances. In order to design the proposed controllers, the following assumptions must be true [17] to [20]:

Hypothesis 1. All the state variables can be measured.

Hypothesis 2. Non-linear functions $f_1(x_1,x_2)$, $f_2(x_1,x_2)$, and $f_3(x_1,x_2,x_6)$ have uncertainty. In other words, $f_i(x) = \hat{f}_i(x) + f_{ui}(x)$ that $\hat{f}_i(x)$ is the known part and $f_{ui}(x)$ is the unknown part of the function $f_i(x)$. Although the dynamics of $f_{ui}(x)$ is unknown, its upper limit is known i.e. $f_{ui}(x) \leq f_i^{max}$.

Hypothesis 3. The nonlinear functions of $g_1(x_1)$, $g_2(x_1)$, and $g_3(x_1)$ are bounded and non-zero. Also, the upper and lower limits of these functions are known, i.e., $0 < g_i^{min} \leq g_{ui}(x) \leq g_i^{max}$.

Hypothesis 4. External disturbances are unknown but have an upper bound, i.e., $\|d_i(t)\| \leq d_i^{max}$.

3. Transferring the dynamic equations of the state space of the system to the error domain

In this part of the article, the dynamic equations of the balanced two-wheeled robot are transferred to the error domain. For this purpose, the following definitions are provided:

$$e_1 = x_1 - x_{d1} \qquad e_4 = x_4 - x_{d4}$$

$$e_2 = x_2 - x_{d2} \qquad e_5 = x_5 - x_{d5} \tag{24}$$
$$e_3 = x_3 - x_{d3} \qquad e_6 = x_6 - x_{d6}$$

That x_{d1} to x_{d6} are the desired paths which must be passed by the variables x_1 to x_6. In the following, derivatives are taken from equations (24) to time, and then equations (23) are inserted into them.

$$\dot{e}_1 = \dot{x}_1 - \dot{x}_{d1} = x_2 - \dot{x}_{d1} \tag{25}$$
$$\dot{e}_2 = \dot{x}_2 - \dot{x}_{d2} = f_1(x_1, x_2) + g_1(x_1)u_1(t) + d_1(t) - \ddot{x}_{d1}$$
$$\dot{x}_{d1} = x_{d2} \rightarrow \ddot{x}_{d1} = \dot{x}_{d2}$$

If the same process is done for all equation (24), the dynamic equations of the balanced two-wheeled robot system in the error field will be as follows:

$$\dot{e}_1 = x_2 - \dot{x}_{d1} = e_2$$
$$\dot{e}_2 = f_1(x_1, x_2) + g_1(x_1)u_1(t) + d_1(t) - \ddot{x}_{d1}$$
$$\dot{e}_3 = x_4 - \dot{x}_{d3} = e_4 \tag{26}$$
$$\dot{e}_4 = f_2(x_1, x_2) + g_2(x_1)u_1(t) + d_2(t) - \ddot{x}_{d3}$$
$$\dot{e}_5 = x_6 - \dot{x}_{d5} = e_6$$
$$\dot{e}_6 = f_1(x_1, x_2, x_6) + g_3(x_1)u_2(t) + d_3(t) - \ddot{x}_{d5}$$

Equation (26) shows the dynamic equations of this system can be divided into two subsystems: under-excitation and full-excitation. The equations of the under-excitation are as follows:

$$\dot{e}_1 = e_2$$
$$\dot{e}_2 = f_1(x_1, x_2) + g_1(x_1)u_1(t) + d_1(t) - \ddot{x}_{d1}$$
$$\dot{e}_3 = e_4 \tag{27}$$
$$\dot{e}_4 = f_2(x_1, x_2) + g_2(x_1)u_1(t) + d_2(t) - \ddot{x}_{d3}$$

The above subsystem is under-excited because it has only input of $u_1(t)$ and its outputs are e_1 and e_3. While the full-excitation subsystem of the following equation has an input of $u_2(t)$ and an output of e_5.

$$\dot{e}_5 = e_6 \tag{28}$$
$$\dot{e}_6 = f_1(x_1, x_2, x_6) + g_3(x_1)u_2(t) + d_3(t) - \ddot{x}_{d5}$$

In the rest of the article and in the controller design section, for the sake of abbreviation, instead of $f_1(x_1,x_2)$, $f_2(x_1,x_2)$, $f_3(x_1,x_2,x_6)$, $g_1(x_1)$, $g_2(x_1)$, $g_3(x_1)$, $d_1(t)$, $d_2(t)$, and $d_3(t)$, f_1, f_2, f_3, g_1, g_2, g_3, d_1, d_2, d_3 are used, respectively.

4. Design the first proposal for SMC

4.1. Design the first proposal SMC for the under-excited subsystem

In this section, the sliding mode controller is designed in such a way that the tracking errors e_1 and e_3 in the sub-excitation subsystem (27) become zero. For this purpose, the following sliding levels are suggested.

$$s_1 = c_1(e_1 - z) + \dot{e}_1$$
$$s_2 = c_2(e_3) + \dot{e}_3 \tag{29}$$

$$z = \varepsilon sat(\frac{s_2}{\emptyset})$$

Where c_1, c_2, and ϕ are positive constants, $0 < \varepsilon < 1$, and sat(*) is the saturation function. The above equations show that if s_1=s_2=0, then we have:

$$\dot{e}_1 + c_1(e_1 - z) = 0 \quad , \quad \dot{e}_3 + c_2(e_3) = 0 \tag{30}$$

According to the above equations, due to over time we will have:

$$e_1 = z \rightarrow \dot{e}_1 = e_2 = 0 \quad , \quad e_3 = 0 \tag{31}$$

Note 1. Since the slip of s_2 has zero, positive or negative values, therefore, based on (29), the variable of z can also be zero, +ε, and −ε. In this case, since 0<ε<1, then variable of z has a constant value in the certain time intervals and as a result $\dot{e}_1 = e_2 = 0$. So, if the slip s_1 and s_2 converge towards zero, it is concluded that:

$$e_1 = z \quad , \quad e_2 = 0 \quad , \quad e_3 = 0 \tag{32}$$

Note 2. Since z= εsat(s_2/ϕ), whenever s_2 = 0 then z = 0, and therefore the tracking error e_1 will also converge to zero.

Theorem 1. In (27) if $u_1(t)$ is chosen as follows, the tracking error e_1, e_2, and e_3 converge to zero asymptotically with any initial conditions.

$$u_1(t) = \frac{1}{\hat{g}_1}\left(-\hat{f}_1 - c_1(e_2 - \dot{z}) + \ddot{x}_{d1}\right) - \rho_1 sign(s_1) \tag{33}$$

That $\hat{g}_1$ and $\hat{f}_1$ are the known dynamics of g_1, f_1, respectively. And ρ_1 is a positive constant.

Proof: The control's input $u_1(t)$ is defined as follows:

$$u_1(t) = u_{eq1}(t) + u_{s1}(t) \tag{34}$$

That $u_{eq1}(t)$ is designed in such a way that if s_1=0, it prevents the changes of the slip surface s_1, while the purpose of designing $u_{s1}(t)$ is to converge the slip surface s_1 to zero. To design $u_{eq1}(t)$, we set the derivative of the sliding surface s_1 equal to zero:

$$\dot{s}_1 = c_1(\dot{e}_1 - \dot{z}) + \ddot{e}_1 = 0 \rightarrow c_1(e_2 - \dot{z}) + \dot{e}_2 = 0 \tag{35}$$

In the above equation, it is concluded that with the passage of time, in order for e_2 to converge to zero, it must become $z = \dot{z} = 0$. Equation (27) is placed in equation (35):

$$\dot{s}_1 = c_1(e_2 - \dot{z}) + f_1(x_1, x_2) + g_1(x_1)u_1(t) + d_1(t) - \ddot{x}_{d1} \rightarrow \tag{36}$$

$$\dot{s}_1 = c_1(e_2 - \dot{z}) + f_1(x_1, x_2) + g_1(x_1)\left(u_{eq1}(t) + u_{s1}(t)\right) + d_1(t) - \ddot{x}_{d1} = 0$$

Now $u_{eq1}(t)$ is chosen as follows:

$$u_{eq1}(t) = \frac{1}{\hat{g}_1}\left(-\hat{f}_1 - c_1(e_2 - \dot{z}) + \ddot{x}_{d1}\right) \tag{37}$$

Which $\hat{g}_1$ and $\hat{f}_1$ are the known dynamics of g_1 and f_1, respectively. By placing (37) in (36), the relation (38) is obtained.

$$\dot{s}_1 = c_1(e_2 - \dot{z}) + f_1 - \frac{g_1}{\hat{g}_1}\hat{f}_1 - \frac{g_1}{\hat{g}_1}c_1(e_2 - \dot{z}) + \frac{g_1}{\hat{g}_1}\ddot{x}_{d1} + g_1 u_{s1}(t) + d_1 - \ddot{x}_{d1} = 0 \tag{38}$$

$$\rightarrow \dot{s}_1 = c_1(e_2 - \dot{z})\left(1 - \frac{g_1}{\hat{g}_1}\right) + f_1 - \frac{g_1}{\hat{g}_1}\hat{f}_1 + \left(\frac{g_1}{\hat{g}_1} - 1\right)\ddot{x}_{d1} + g_1 u_{s1}(t) + d_1 = 0$$

$$\dot{s}_1 = c_1(e_2 - \dot{z})\left(1 - \frac{g_1}{\hat{g}_1}\right) + f_1 - \frac{g_1}{\hat{g}_1}\hat{f}_1 + \left(\frac{g_1}{\hat{g}_1} - 1\right)\ddot{x}_{d1} + d_1 + (g_1 - 1)u_{s1}(t) + u_{s1}(t) = 0$$

In the following η is defined as (39):

$$\eta = c_1(e_2 - \dot{z})\left(1 - \frac{g_1}{\hat{g}_1}\right) + f_1 - \frac{g_1}{\hat{g}_1}\hat{f}_1 + \left(\frac{g_1}{\hat{g}_1} - 1\right)\ddot{x}_{d1} + d_1 + (g_1 - 1)u_{s1}(t) \tag{39}$$

Note 3. In fact, η is the sum of all the structural and non-structural uncertainties in the dynamic equations of the under-excitation subsystem.

$$\dot{s}_1 = \eta + u_{s1}(t) = 0 \tag{40}$$

To design of $u_{s1}(t)$, the Lyapunov candidate function is suggested below:

$$V_1(s_1) = \frac{1}{2}s_1^2 \tag{41}$$

From the above equation, we get a derivative to time:

$$\dot{V}_1(s_1) = s_1\dot{s}_1 = s_1(\eta + u_{s1}(t)) \tag{42}$$

Now $u_{s1}(t)$ is selected as follows:

$$u_{s1}(t) = -\rho_1 sign(s_1) \tag{43}$$

which ρ_1 is a positive constant. By substituting (43) in (42), we will have:

$$\dot{V}_1(s_1) = s_1\big(\eta - \rho_1 sign(s_1)\big) = s_1\eta - \rho_1\frac{s_1^2}{|s_1|} = s_1\eta - \rho_1|s_1| \tag{44}$$

In the above equation, $\dot{V}_1(s_1) \leq 0$ when $\rho_1 > |\eta|$, and $\dot{V}_1(s_1) = 0$ when s_1=0. Therefore, according to Lassalle's theorem, with the selection of $u_{s1}(t)$ and the appropriate selection of the coefficient ρ_1, $\dot{V}_1(s_1)$ becomes smaller than zero and as a result, s_1 converges to zero [35]. When the slip surface s_1 becomes zero based on (30), e_1=z and e_2=0. On the other hand, based on (35), when $z = \dot{z} = 0$ then e_2=0. Since z= εsat(s_2/ϕ), z will be zero if s_2=0, so we conclude that when e_2 becomes zero, e_1=z=s_2=0. Then, when s_2 becomes zero, e_3 also becomes zero with the passage of time.

According to (34), (37) and (43), it is concluded that $u_1(t)$ has the following form:

$$u_1(t) = \frac{1}{\hat{g}_1}\left(-\hat{f}_1 - c_1(e_2 - \dot{z}) + \ddot{x}_{d1}\right) - \rho_1 sign(s_1) \tag{45}$$

4.2. Design the first SMC for the full-excited subsystem

In this part of the article, the sliding mode controller is designed in such a way that the tracking error e_5 in the full-excited subsystem (28) becomes zero.

Theorem 2. In the subsystem (28), if $u_2(t)$ will be chosen as follows, the tracking errors e_5 and e_6 converge to zero asymptotically with any initial conditions.

$$u_2(t) = \frac{1}{\hat{g}_3}\left(-\hat{f}_3 - c_1 e_6 + \ddot{x}_{d5}\right) - \rho_2 sign(s_3) \tag{46}$$

$$s_3 = c_3 e_5 + \dot{e}_5$$

That c_3 and ρ_2 are positive constants. Also, $\hat{g}_3$ and $\hat{f}_3$ are the known dynamics of g_3 and f_3, respectively.

Proof. Since the process of proving this case is the same as the proof of theorem 1, it is omitted in this section.

Note 4. Since a sliding surface is defined for the full-excited subsystem (28), therefore, to prove theorem 2, there is no need to define the variable z anymore, and for this reason, proving theorem 2 is easier than theorem 1.

4.3. Proving the stability of the first SMC

In (26), if we choose $u_1(t)$ and $u_2(t)$ using (33) and (46), respectively, based on theorems (1) and (2), the under-excited and full-excited subsystems of equations (27) and (28) are stable and then the tracking errors e_1, e_2, e_3, e_4, e_5, and e_6 converge to zero with any initial conditions in the presence of existing uncertainties. Therefore, the system has global asymptotic stability.

5. Design the second proposal for SMC

5.1. The design of the second SMC for control of the under-excited subsystem

In this part of the article, another sliding mode controller is proposed to control the under-excited subsystem (27). For this purpose, the following slip surfaces are defined:

$$s_1 = \lambda_1 e_1 + e_2 \tag{47}$$
$$s_2 = \lambda_2 e_3 + e_4$$

That, λ_1 and λ_2 are positive constants. According to the design method of the previous section, the equivalent inputs of this subsystem can be obtained as follows:

$$u_{eq1}(t) = \frac{1}{\hat{g}_1}\left(-\hat{f}_1 - \lambda_1 e_2 + \ddot{x}_{d1}\right) \tag{48}$$
$$u_{eq2}(t) = \frac{1}{\hat{g}_2}\left(-\hat{f}_2 - \lambda_2 e_4 + \ddot{x}_{d3}\right)$$

Theorem 3. In the subsystem of (27), if $u_1(t)$ is chosen as follows, the tracking error e_1, e_2, and e_3 converge to zero asymptotically with any initial conditions.

$$u_1(t) = u_{eq1}(t) + u_{eq2}(t) + u_s(t) \tag{49}$$
$$u_s(t) = \frac{-1}{(\gamma \hat{g}_2 + \alpha \hat{g}_1)} \times [\gamma \hat{g}_2 u_{eq1}(t) + \alpha \hat{g}_1 u_{eq2}(t) + ks + \rho_3 sign(s)]$$

Where k, γ, α, and ρ_3 are positive constants.

Proof. To prove theorem 3, slip surface S is considered as a combination of slip surfaces s_1 and s_2.

$$S = \alpha s_1 + \gamma s_2 \tag{50}$$

Where α and γ are constant coefficients. The following Lyapunov candidate function is proposed to design the input $u_s(t)$:

$$V(S) = \frac{1}{2} S^2 \tag{51}$$

We derive the Lyapunov candidate function with respect to time and:

$$\dot{V}(s) = S\dot{S} = S[\alpha(\lambda_1\dot{e}_1 + \dot{e}_2) + \gamma(\lambda_2\dot{e}_3 + \dot{e}_4)] \quad (52)$$

Equations (27), (48) and (49) are replaced in (52).

$$\dot{V}(s) = S\dot{S} = S[\alpha(\lambda_1\dot{e}_1 + \dot{e}_2) + \gamma(\lambda_2\dot{e}_3 + \dot{e}_4)] \quad (53)$$

$$\dot{V}(s) = S\dot{S} = S\big[\alpha\big(\lambda_1 e_2 + \hat{f}_1 + \hat{g}_1\big(u_{eq1} + u_{eq2} + u_s\big) + d_1\big) + \gamma\big(\lambda_2 e_4 + \hat{f}_2 + \hat{g}_2\big(u_{eq1} + u_{eq2} + u_s\big) + d_2\big)\big] =$$

$$S[\alpha\lambda_1 e_2 + \alpha\hat{f}_1 + \alpha\hat{g}_1 u_{eq1} + \alpha\hat{g}_1\big(u_{eq2} + u_s\big) + \gamma\lambda_2 e_4 + \gamma\hat{f}_2 + \gamma\hat{g}_2 u_{eq2} + \gamma\hat{g}_2\big(u_{eq2} + u_s\big) + \alpha d_1\gamma d_2] =$$

$$S\big[\alpha\hat{g}_1\big(u_{eq2} + u_s\big) + \gamma\hat{g}_2\big(u_{eq2} + u_s\big) + \alpha d_1\gamma d_2\big] =$$

$$S[(\gamma\hat{g}_2 u_{eq1} + \alpha\hat{g}_1 u_{eq2} + u_s(\gamma\hat{g}_2 + \alpha\hat{g}_1) + \alpha d_1 + \gamma d_2]$$

$$u_s(t) = \frac{-1}{(\gamma\hat{g}_2 + \alpha\hat{g}_1)} \times [\gamma\hat{g}_2 u_{eq1}(t) + \alpha\hat{g}_1 u_{eq2}(t) + ks + \rho_3 sign(s)] \quad (54)$$

Where k and ρ_3 are positive constants. By substituting (54) in (53), we have:

$$\dot{V}(S) = S[-ks - \rho_3 sign(s) + \alpha d_1 + \gamma d_2] = -kS^2 - \rho_3|S| + S(\alpha d_1 + \gamma d_2) \leq -kS^2 - \rho_3|S| + S(\alpha D_1 + \gamma D_2) \quad (55)$$

It can be concluded from (55) that with the appropriate selection of coefficients α, ρ_3, k, and γ, the derivative of the Lyapunov function becomes smaller than zero. Therefore, the sliding surface S converges to zero with the passage of time.

Note 5. Equation (55) shows that by properly choosing the coefficients α, ρ_3, k, and γ, it is possible to converge the sliding surface S towards zero. Zeroing of slip surface S does not necessarily lead to zeroing of slip surfaces s_1 and s_2. Therefore, the zeroing of the slip surface S does not guarantee the proof of the stability of the subsystem (27).

5.2. Stability analysis of the under-excited subsystem with application of second SMC

In the previous section, it was proved that the control input with (47) to (50) converges the sliding surface S to zero in the presence of existing structural and non-structural uncertainties. In this section, we want to prove that the zeroing of the slip surface S causes the zeroing of the slip surfaces s_1 and s_2, and finally the under-excited subsystem has global asymptotic stability and theorem 3 is proved.

To analyze the stability of the under-excited subsystem, we take the integral from both sides (55) with respect to time:

$$\int_0^t \dot{V}dt = \int_0^t \big(-kS^2 - \rho_3|S| + S(\alpha D_1 + \gamma D_2)\big)dt \quad (56)$$

$$V(t) - V(0) = \int_0^t (-\rho_3 - (\alpha D_1 + \gamma D_2))|S| - kS^2)dt$$

In the following, we have (57) from (51) and (56).

$$V(S) = \frac{1}{2}S^2 = V(0) - \int_0^t (\rho_3 - (\alpha D_1 + \gamma D_2))|S| + kS^2)dt \leq V(0) < \infty \quad (57)$$

It follows from (57) that S∈L∞. In other words:

$$\sup_{t\geq 0}|S| = \|S\|_\infty < \infty \quad (58)$$

From (55) and (58) we will have:

$$\dot{V}(s) = S\dot{S} \leq -kS^2 - \rho_3|S| + |S|(\alpha D_1 + \gamma D_2) < \infty \quad (59)$$

It is concluded from the above equation that $\dot{S} \in L_\infty$. It means:

$$\sup_{t\geq 0}|\dot{S}| = \|\dot{S}\|_\infty < \infty \quad (60)$$

Therefore, it follows from (58) and (60) that:

$$\sup_{t\geq 0}|S_1| = \|S_1\|_\infty < \infty \quad , \quad \sup_{t\geq 0}|\dot{S}_1| = \|\dot{S}_1\|_\infty < \infty \quad (61)$$

$$\sup_{t\geq 0}|S_2| = \|S_2\|_\infty < \infty \quad , \quad \sup_{t\geq 0}|\dot{S}_2| = \|\dot{S}_2\|_\infty < \infty$$

According to the above information, we know that if $\rho_3 > (\alpha D_1 + \gamma D_2)$, then the values of α and γ do not have a direct effect on the stability of the system. Therefore, the following two slip surfaces are introduced:

$$S_1 = (\alpha_1 s_1 + \gamma s_2) \quad (62)$$

$$S_2 = (\alpha_2 s_1 + \gamma s_2)$$

That α_1 and α_2 are the arbitrary constants and it is assumed that $\alpha_1 \neq \alpha_2$, so $S_1 \neq S_2$. It is also assumed that $0 < \int_0^\infty s_2^2 dt < \int_0^\infty s_1^2 dt < \infty$. So, according to (57), we will have:

$$0 \leq \int_0^\infty s_1^2 dt = \int_0^\infty (\alpha_1^2\alpha_2^2 + 2\alpha_1\gamma^2 s_1 s_2 + \gamma^2 s_2^2)dt < \infty \quad (63)$$

$$0 \leq \int_0^\infty s_2^2 dt = \int_0^\infty (\alpha_1^2\alpha_2^2 + 2\alpha_1\gamma^2 s_1 s_2 + \gamma^2 s_2^2)dt < \infty$$

So:

$$0 < \int_0^\infty (S_1^2 - S_2^2)dt = \int_0^\infty ((\alpha_1^2 - \alpha_2^2)s_1^2 + 2(\alpha_1 - \alpha_2)\gamma s_1 s_2)dt < \infty \quad (64)$$

And, then:

$$= \int_0^\infty ((\alpha_1^2 - \alpha_2^2)s_1^2 + 2(\alpha_1 - \alpha_2)\gamma s_1 (S_1 - \alpha_1 s_1))dt = \quad (65)$$

$$\int_0^\infty -(\alpha_1 - \alpha_2)^2 s_1^2 dt + \int_0^\infty 2(\alpha_1 - \alpha_2)\, s_1 S_1 dt > 0$$

According to (57):

$$\int_0^\infty ((\rho_3 - (\alpha D_1 + \gamma D_2))\,|S| + kS^2)dt = \tag{66}$$

$$\int_0^\infty (\rho_3 - (\alpha D_1 + \gamma D_2))\,|S|dt + \int_0^\infty kS^2\,dt \le V(0) < \infty$$

Since $\rho_3 > (\alpha D_1 + \gamma D_2)$ and k>0, therefore $\int_0^\infty kS^2\,dt \ge 0$ and $\int_0^\infty (\rho_3 - (\alpha D_1 + \gamma D_2))\,|S|dt \ge 0$. Because the sum of two positive values is a finite value, therefore each of these positive values will be finite. So, $0 \le \int_0^\infty \big(\rho_3 - (\alpha D_1 + \gamma D_2)\big)\,|S|dt = \|S\|_1 \le \infty$, i.e., $S \in L_1$. In the following, we will have from (65):

$$\int_0^\infty (\alpha_1 - \alpha_2)^2\, s_1^2 dt < \int_0^\infty 2(\alpha_1 - \alpha_2)\, s_1 S_1 dt \le \tag{67}$$

$$2\int_0^\infty |\alpha_1 - \alpha_2|\, s_1 S_1 dt \le 2|\alpha_1 - \alpha_2| \int_0^\infty \|s_1\|_\infty |S_1|dt =$$

$$2|\alpha_1 - \alpha_2|\|s_1\|_\infty |S_1| < \infty$$

According to (67), we have:

$$\int_0^\infty s_1^2 dt < \infty \tag{68}$$

In a similar way, it is proved that:

$$\int_0^\infty s_2^2 dt < \infty \tag{69}$$

It follows from (68) and (69) that $s_1 \in L_1$ and $s_2 \in L_2$. Since $s_1 \in L_\infty$, $\dot{s}_1 \in L_\infty$, $\dot{s}_2 \in L_\infty$, and $s_2 \in L_\infty$, therefore, based on Barbalat's lemma, it can be concluded that $\lim_{t\to\infty} s_1 = 0$, $\lim_{t\to\infty} s_2 = 0$, and theorem 3 is proved [35]. The second final proposed sliding mode control for under-excited subsystem (27) is given below:

$$\begin{cases} u_1(t) = u_{eq1}(t) + u_{eq2}(t) + u_s(t) \\ u_{eq1}(t) = \dfrac{1}{\hat{g}_1}\left(-\hat{f}_1 - \lambda_1 e_2 + \ddot{x}_{d1}\right) \\ u_{eq2}(t) = \dfrac{1}{\hat{g}_2}\left(-\hat{f}_2 - \lambda_2 e_4 + \ddot{x}_{d3}\right) \\ u_s(t) = \dfrac{-1}{(\gamma\hat{g}_2 + \alpha\hat{g}_1)} \times \\ [\gamma\hat{g}_2 u_{eq1}(t) + \alpha\hat{g}_1 u_{eq2}(t) + ks + \rho_3 sign(s)] \end{cases} \tag{70}$$

5.3. Proving the stability of the closed loop system using the second SMC for the under-excited subsystem

In (26), if we choose $u_1(t)$ and $u_2(t)$ according to (70) and (46), respectively, based on theorems of 3 and 2, under-excited and full-excited subsystems (27) and (28) are stable and the tracking errors e_1, e_2, e_3,

e_4, e_5, and e_6 will converge to zero with any initial conditions in the presence of existing uncertainties, and therefore the closed loop system will have global asymptotic stability.

6. Advantages and disadvantages of the first and second controllers of under-excited subsystem

The proposed first and second sliding mode controllers of under-excited subsystem have advantages and disadvantages that are mentioned below:

- Proving the stability of theorem 1, in other words, the under-excited subsystem in the presence of the first proposed sliding mode control, is highly dependent on the value of the variable of z. Since $z = \varepsilon sat(s_2/\phi)$, it follows that the value of this variable depends on the correct selection of the coefficient ε. As mentioned in section 3, the value of this coefficient is chosen as $0<\varepsilon<1$. If the value of this coefficient is chosen very close to 1, the variable z will converge towards zero later and this will cause the analysis process between the state variables of the under-excited subsystem to not be done completely and this will cause the steady state's error in the tracking desired routes in this subsystem. But if we approach the value of this coefficient to zero, the analysis process is completely done and no steady state error will be observed.
- The number of input coefficients of the first proposed sliding mode control is less than the second proposed sliding mode control coefficients and the adjustment of these coefficients is much easier because in the second proposed sliding mode control α and γ are constant coefficients. Therefore, the values of these coefficients can be positive or negative. In this case, it is difficult to adjust these coefficients by using the trial-and-error method.
- If the input coefficients of the proposed controllers are well adjusted, the analysis process among the state variables in the under-excited subsystem is performed more fully through the first proposed sliding mode control. For this reason, the performance of this controller is more favorable in overcoming structural and non-structural uncertainties and external disturbances. This case is fully shown in the simulations section.
- To implement the first proposed sliding mode control, access to the known dynamics g_1 and f_1 is enough, while to implement the second proposed sliding mode control, access to the known dynamics f_1, f_2, g_1, and g_2 is necessary. This greatly increases the volume of calculations and the maximum input range of the second proposed sliding mode control.
- By implementing the proposed sliding mode controllers, the dynamic control of the balanced two-wheel robot system is done completely and there is no need to use the kinematic control method in this system. Therefore, the presence of other structural uncertainties cannot have an effect on the stability of the closed loop system and the tracking error.

7. Simulation Verifications

In this part of the article, to investigate the performance of the proposed controllers, simulations are implemented in several stages on the balanced two-wheel robot system. In carrying out the simulations, we tried to make the proposed controllers face a more serious challenge in each stage so that we would be able to examine and compare their performance. To perform the simulations, the parameters of the balanced two-wheel robot system were set equal to the values in table 1. The initial conditions of the state variables of this system were considered as $x_1(0)=\pi/180$ and the rest of them were considered as zero. The optimal direction of the state variables was chosen equal to $x_{d1}=0$ and $x_{d2}= \pi/2$. It should be mentioned that for the x_3 state variable, in order to create basic challenges for the proposed controllers and to examine their performance more precisely, different optimal paths have been selected in the 3-stage simulations. The coefficients of the first and second proposed controllers are listed in tables 2 and 3, respectively. In all stages of the simulations, to prevent the occurrence of vibration in the control input, the method of creating a boundary layer around the zero-slip surface has been used.

Table 2. The coefficients of the first proposed sliding mode control of the under-excited and full-excited subsystem.

Coefficient	Value
C_1	15
C_2	0.45
C_3	20
ρ_1	5
ρ_2	6
ε	0.42
ϕ	12

Table 3. The coefficients of the second proposed sliding mode control of the under-excited and full-excited subsystem.

Coefficient	Value
λ_1	2.8
λ_2	0.6
C_3	20
ρ_2	6
ρ_3	4
α	0.45
γ	1
k	3

7.1. The first stage of the Simulation

In this part of the simulation, the performance of the proposed controllers is investigated only in the presence of structural uncertainties, and non-structural uncertainties such as external disturbances are considered zero. In order to apply structural uncertainties, it was assumed in the design of the proposed controllers that the values of the balanced two-wheel robot system parameters are 85% of the values in table 1. In this way, the proposed controllers face 15% estimation error in system parameters.

After running the simulation, it can be concluded from figures (2.a) and (2.b) that the first and second proposed sliding mode controllers have worked well and have converged the state variables of the under-excited subsystem towards the desired values. From these figures, it can be concluded that the performance of the proposed controllers in controlling this subsystem is very close to each other, and only at the beginning of the control process, it can be seen that the x_1 and x_3 state variables have maximum changes by applying the second proposed sliding mode control.

Note 6. It can be seen carefully in Figures (2.a) and (2.b) that the performance of the proposed controllers is such that the x_1 and x_3 state variables have converged to the desired values in times equal to 8 and 30 seconds, respectively. The reason for the slowness of this time response goes back to the selection of the initial conditions of the x_3 state variable. As mentioned, $x_3(0)=0$, but as it can be seen in Figure (2.b), at the moment of starting the simulation process, the tracking error size of e_3 is equal to 1 meter. For this reason, the proposed controllers need a lot of time to reduce and ultimately make the tracking error zero, and this increases the time response of the controllers. Therefore, it is clear that if the initial conditions of the x_3 state variable are closer to the desired path, the time response of the proposed controllers becomes faster.

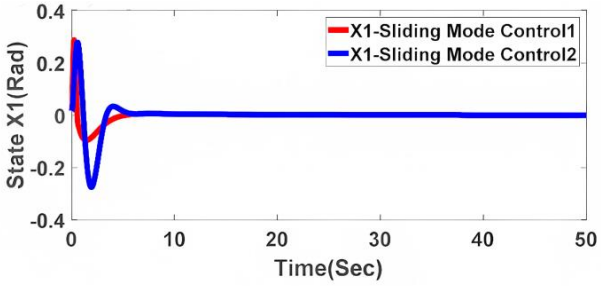

Fig 2.a. The behavior of state x_1 of the under-excited subsystem by applying the first and second proposed sliding mode controllers in the presence of structural uncertainties.

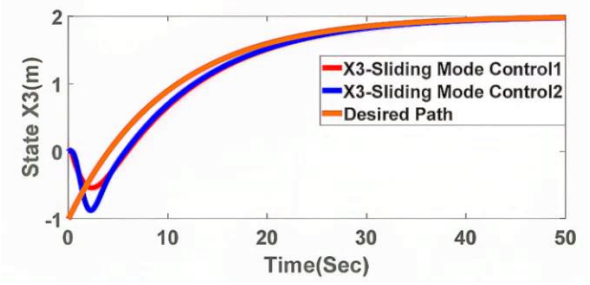

Fig 2.b. The behavior of state x_3 of the under-excited subsystem by applying the first and second proposed sliding mode controllers in the presence of structural uncertainties.

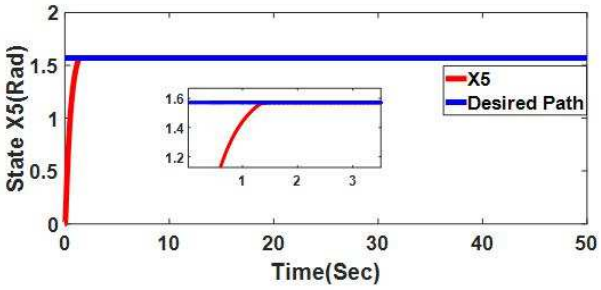

Fig 2.c. The behavior of state x_5 of the full-excited subsystem by applying the first and second proposed sliding mode controllers in the presence of structural uncertainties.

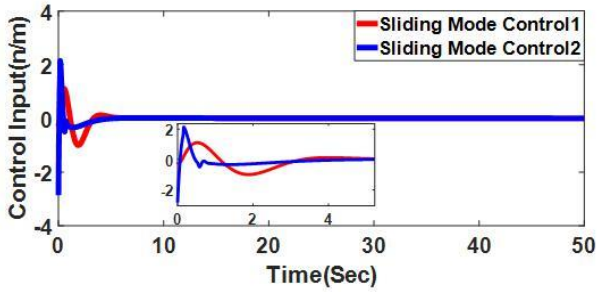

Fig 2.d. The control's input of the under-excited subsystem by applying the first and second proposed sliding mode controllers in the presence of structural uncertainties.

It can be seen in figure (2.c) that the proposed sliding mode control of the subsystem has controlled all the excitation well and has brought the x_5 state variable to the desired value in a time equal to 1.5 seconds. It can be concluded from figure (2.d) that although the performance of the proposed controllers in the control of the under-excited subsystem is very close to each other, the maximum control range of the second proposed sliding mode is approximately 2.5 times the maximum control range of the first proposed sliding mode. In Figure (2.e), we can see that the control of the full-excited subsystem is done with a maximum range of 1 N/m. Although the initial conditions of the state variable x_5 equal to zero radians are selected and the proposed controllers for transferring the balanced two-wheel robot system from the lying down state to the upright state need to spend more energy, but from figures (2.d) and (2.e) it can be concluded that the maximum input range of the controls are within an acceptable range.

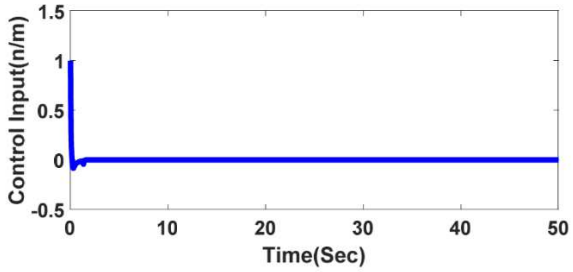

Fig 2.e. The control's input of the full-excited subsystem by applying the proposed sliding mode controllers in the presence of structural uncertainties.

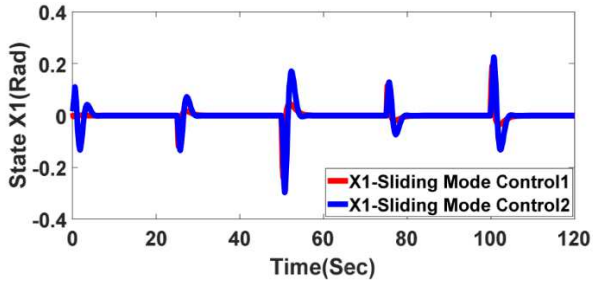

Fig 2.f. Variable behavior of the x_1 state of the under-excitation subsystem by applying the first and second proposed sliding mode controllers in the presence of structural uncertainties and time-constant external disturbances.

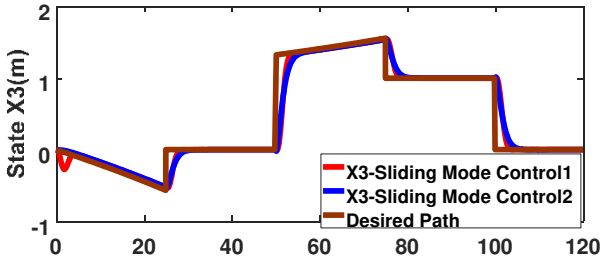

Fig 2.g. Variable behavior of the x_3 state of the under-excited subsystem by applying the first and second proposed sliding mode controllers in the presence of structural uncertainties and time-invariant external disturbances.

7.2. The second stage of the Simulation

In this part of the simulation, the proposed controllers face more challenges. For this purpose, in addition to the structural uncertainties of the first stage of simulation, the balanced two-wheel robot system is exposed to constant external disturbances with a time equal to $d_1(t)=d_2(t)=d_3(t)=0.03$. In addition, a variable path with uneven time was selected for the two-wheeled robot system. The initial conditions of the variables of the objective state were set equal to the simulation of the first stage.

After running the simulation, it can be concluded from figures (2.f) and (2.g) that the proposed controllers have performed well in controlling the under-excited subsystem, and in addition to being able to keep the balanced two-wheel robot system in an upright position, they have also made the robot follow the desired path well trace carefully in these figures, we can see that in the uneven parts of the path, the balance of the robot fluctuates, but the proposed controllers work well and prevent the balance of this robot from getting upset. It should be noted that the variable behavior of the x_1 state with the application of the first proposed sliding mode control has a lower fluctuation range, but the difference in the variable behavior of the x_3 state is not very noticeable in the presence of the proposed controllers. In figure (3.a), it can be seen that the control process of the full drive subsystem is well done and the proposed sliding mode control has converged the x_5 state variable to the desired value in the presence of uncertainties in 1.5 seconds. It can be concluded from figure (3.b) that the proposed controllers have to spend more energy to maintain the balance of the two-wheel robot system in the presence of existing uncertainties and uneven time-varying path. But carefully in this figure, we find out that the optimal performance of the second proposed sliding mode control is associated with a very large maximum range. By comparing figures (2.f), (2.g) and (3.b), it can be concluded that although the performance of

the proposed controllers in controlling x_1 and x_3 is very close to each other, a 4 times difference in their maximum range cannot be ignored. In figure (5.a), it can be seen that the sliding mode control proposed for the control of the full propulsion subsystem faces more challenges and has a maximum range of 2 N/m to maintain the variable position of the x_5 mode.

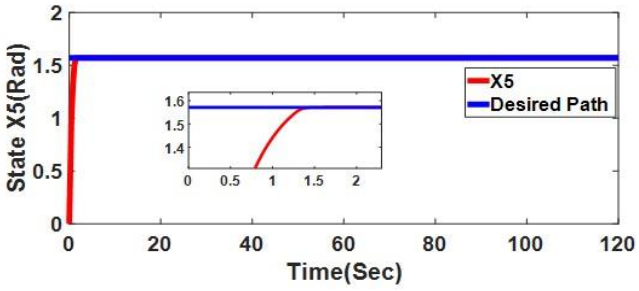

Fig 3.a. Variable behavior of the x_5 state of the under-excited subsystem by applying the first and second proposed sliding mode controllers in the presence of structural uncertainties and time-constant external disturbances.

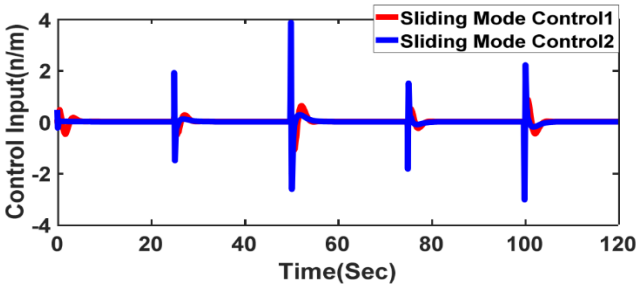

Fig 3.b. The control's input of the under-excited subsystem by applying the first and second proposed sliding mode controllers in the presence of structural uncertainties and time-constant external disturbances.

7.3. The third stage of the Simulation

In this part of the simulation, the performance of the proposed controllers in dealing with more basic challenges is investigated. For this purpose, in addition to the structural uncertainties in the first and second stage simulations, the balanced two-wheel robot system is exposed to variable external disturbances with a time equal to $d_1(t)=d_2(t)=d_3(t)=0.05\sin(0.3t)$. At this stage, the robot system must go through the time-varying and uneven path of the second stage of simulation, and during this path, successive flips are used to disturb its balance. The flips that are applied to the balanced two-wheel robot system can move this system away from the vertical position up to 0.2 radians, and the duration of their application is equal to 1 second. The initial conditions of the state variables were exactly equal to their values in the first and second stage simulations.

After running the simulation, it can be concluded from figures (4.b) and (4.c) that the control performance of the first proposed sliding mode is very good in overcoming the existing structural and non-structural uncertainties and the jerk that is applied to the robot system. In figure (4.b), we can see that with each flip, the maximum range of fluctuations of the x_1 state variable reaches 1.2 radians as a result of applying the second proposed sliding mode control, while the first proposed sliding mode control reduces the maximum range of fluctuations of this state variable. It has decreased from 0.5 radians. In figure (4.c), it can be seen that the flip applied to the two-wheel robot system, the control of

the second proposed sliding mode has faced a great challenge, so that in the 67th second, the x_3 state variable is separated by approximately 4 meters from the desired path. While the first proposed sliding mode control has reduced the changes of this state variable to less than 1 meter. In figure (4.d), we can see that the performance of the proposed control in the control of the whole excitation subsystem is very favorable, and the existing uncertainties and successive flips do not have an effect on the 5x state variable control process. From Figure (4.e), it can be concluded that the unfavorable performance of the sliding mode controls the second proposal faces a maximum range equal to 4 N/m, which is more than 4 times the maximum range of the sliding mode control of the first proposal. In figure (4.f), it can be seen that the optimal performance of the proposed sliding mode control of the full excitation subsystem has a maximum range of 2 N/m, which is within an acceptable range in the presence of existing uncertainties and successive jerks.

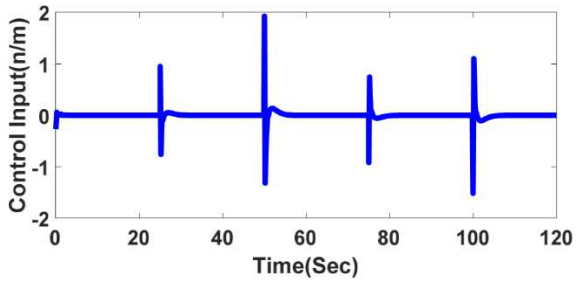

Fig 4.a. The control's input of the full-excited subsystem by applying the first and second proposed sliding mode controllers in the presence of structural uncertainties and time-constant external disturbances.

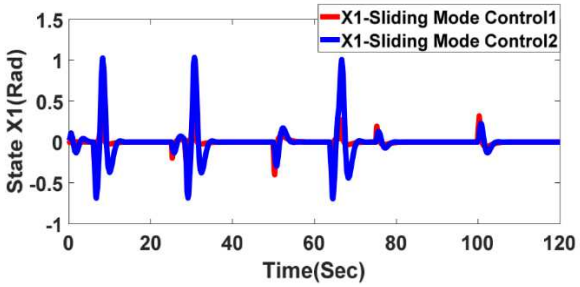

Fig 4.b. Variable behavior of the x_1 state of the under-excitation subsystem by applying the first and second proposed sliding mode controllers in the presence of structural uncertainties and time-constant external disturbances and consecutive flips.

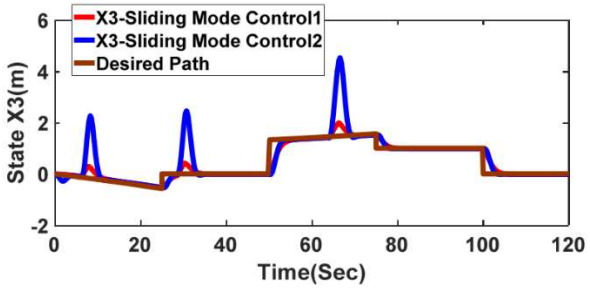

Fig 4.c. Variable behavior of the x_3 state of the under-excitation subsystem by applying the first and second proposed sliding mode controllers in the presence of structural uncertainties and time-constant external disturbances and consecutive flips.

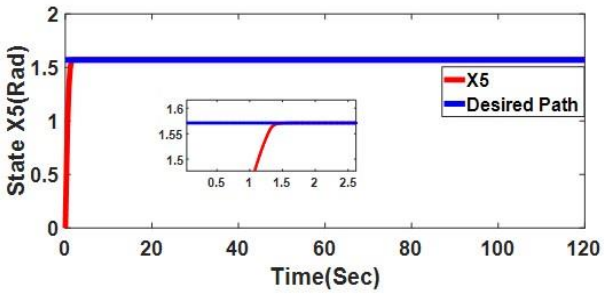

Fig 4.d. Variable behavior of the x_5 state of the under-excitation subsystem by applying the first and second proposed sliding mode controllers in the presence of structural uncertainties and time-constant external disturbances and consecutive flips.

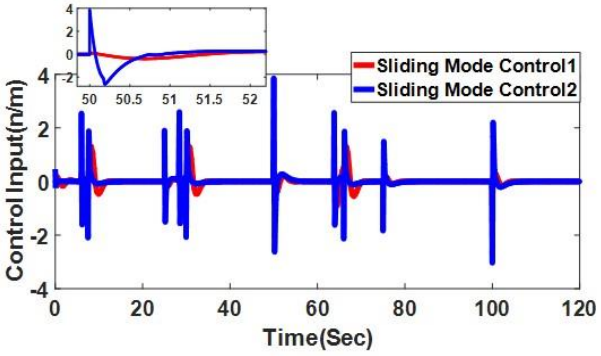

Fig 4.e. The control's input of the under-excited subsystem by applying the first and second proposed sliding mode controllers in the presence of structural uncertainties and time-constant external disturbances and consecutive flips.

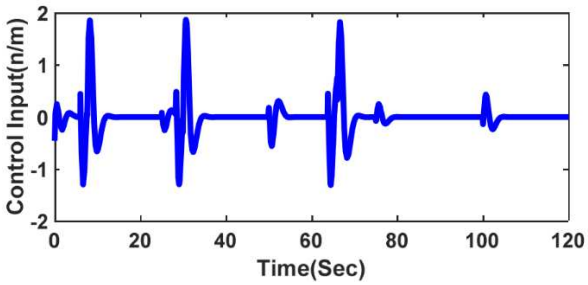

Fig 4.f. The control's input of the full-excited subsystem by applying the first and second proposed sliding mode controllers in the presence of structural uncertainties and time-constant external disturbances and consecutive flips.

7.4. The results of the simulations

From the presented 3-stage simulations and the data in tables 4 to 6, the following results are obtained:

Table 4. Comparing the performance of the proposed controllers in the first stage simulation

	First-stage simulation in the presence of structural uncertainties			
	The maximum overshoot of x_1	*The maximum overshoot of* x_3	*The maximum overshoot of* x_5	*The maximum domain of the control's input*
First proposed sliding mode control for under-excited subsystem	1 rad	0.5 m	-	1 N/m
Second proposed sliding mode control for under-excited subsystem	0.3 rad	0.8 m	-	2.2 N/m
Full-excited subsystem	-	-	0	1 N/m

Table 5. Comparing the performance of the proposed controllers in the second stage simulation

Second stage simulation in the presence of structural uncertainties and time constant external disturbances				
	The maximum overshoot of x_1	*The maximum overshoot of* x_3	*The maximum overshoot of* x_5	*The maximum domain of the control's input*
First proposed sliding mode control for under-excited subsystem	0.25 rad	0.25 m	-	0.3 N/m
Second proposed sliding mode control for under-excited subsystem	0.3 rad	0	-	4 N/m
Full-excited subsystem	-	-	0	1.9 N/m

Table 6. Comparing the performance of the proposed controllers in the third stage simulation

Second stage simulation in the presence of structural uncertainties and time constant external disturbances and successive flips				
	The maximum overshoot of x_1	*The maximum overshoot of* x_3	*The maximum overshoot of* x_5	*The maximum domain of the control's input*
First proposed sliding mode control for under-excited subsystem	0.3 rad	0.9 m	-	0.4 N/m
Second proposed sliding mode control for under-excited subsystem	1.1 rad	0.9 m	-	4 N/m
Full-excited subsystem	-	-	0	1.9 N/m

1) If relatively accurate information is available from the dynamic equations of the balanced two-wheel robot system, this will reduce the existing uncertainties. As a result, the input coefficients of the proposed controllers related to the sub-excitation subsystem can be adjusted in such a way that they perform very close to each other.
2) In case of non-structural uncertainties such as external disturbances, if the limit of these uncertainties is not too high, it is possible to provide similar performance to each other through proper adjustment of the input coefficients of the proposed under-excited subsystem controllers. But in this situation, the maximum control range of the second proposed sliding mode is much larger, and in this case, high power drives should be used in the balanced two-wheel robot system. This increases the economic costs of the practical implementation of the second proposed sliding mode control.
3) In the event of external disturbances with a high maximum amplitude, the performance of the second proposed sliding mode control in the control of the under-excited subsystem faces a great challenge and cannot well prevent the fluctuations of the state variables of this subsystem. The reason for this is due to the sliding surfaces that are defined for this subsystem. Since the slip surface S is a linear combination of the slip surfaces s_1 and s_2, therefore, if the uncertainty limits are large, it will affect the oscillatory behavior of at least one of these slip surfaces. As a result, the discontinuous part of the control input, which is a function of the slip surface S,

cannot be very effective in reducing the maximum range of fluctuations of the state variables related to that slip surface.

4) The occurrence of structural and non-structural uncertainties and external disturbances have a great impact on the performance of the sub-excitation subsystem controller, but the effect of these uncertainties on the performance of the full-excitation subsystem controller is less.

8. Conclusion

In this article, solutions were proposed to control the balanced two-wheel robot system in the presence of structural and non-structural uncertainties. In order to design the proposed controllers, at first, the dynamic equations of the balanced two-wheel robot system were divided into two subsystems, under-excited and full-excited, and then two different methods were proposed to control the under-excited subsystem based on sliding mode control. In the design of the first proposed sliding mode control, two slip surfaces were defined and the variable of z was used to establish a connection between these surfaces. After that, the control's input was designed in such a way that the variable of z and the slip surfaces converge to zero in the presence of existing uncertainties. But in the second proposed sliding mode control design method, a third sliding surface was used to establish a connection between the slip surfaces, which is a linear combination of the first and second slip surfaces. In the following, the proposed control's input was designed in such a way that the third slip surface converges to zero in the presence of existing uncertainties, and it was proved that the zeroing of the third slip surface also converges the first and second slip surfaces to zero. Sliding mode control was also proposed to control the full-excited subsystem, which made it have global asymptotic stability in the presence of existing structural and non-structural uncertainties. Since the under-excited and full-excited subsystems are independent of each other, therefore the overall asymptotic stability of both subsystems follows the overall asymptotic stability of the system. In the following, the advantages and disadvantages of the proposed solutions were mentioned, and after that, to show the performance of the proposed controllers, simulations were implemented in 3 stages on the balanced two-wheel robot system. In presenting the proposed simulations, an effort was made to expose the proposed controllers to more serious challenges step by step, so that their performance compared to each other can be fully determined.

References

[1] Mohareri, O., Dhaouadi, R. and Rad, A.B. (2012). Indirect adaptive tracking control of a nonholonomic mobile robot via neural networks. *Neurocomputing*, 88, pp.54–66. doi:https://doi.org/10.1016/j.neucom.2011.06.035.

[2] Villarreal-Cervantes, M.G., Guerrero-Castellanos, J.F., Ramírez-Martínez, S. and Sánchez-Santana, J.P. (2015). Stabilization of a (3,0) mobile robot by means of an event-triggered control. *ISA Transactions*, 58, pp.605–613. doi:https://doi.org/10.1016/j.isatra.2015.06.013.

[3] Miah, M.S. and Gueaieb, W. (2014). Mobile robot trajectory tracking using noisy RSS measurements: An RFID approach. *ISA Transactions*, 53(2), pp.433–443. doi:https://doi.org/10.1016/j.isatra.2013.09.016.

[4] Scaglia, G.J.E., Serrano, M.E., Rosales, A. and Albertos, P. (2015). Linear interpolation based controller design for trajectory tracking under uncertainties: Application to mobile robots. *ri.conicet.gov.ar*. [online] doi:https://doi.org/10.1016/j.conengprac.2015.09.010.

[5] Baloh, M., & Parent, M. (2003, December). Modeling and model verification of an intelligent self-balancing two-wheeled vehicle for an autonomous urban transportation system. In *The conference on computational intelligence, robotics, and autonomous systems* (pp. 1-7).

[6] Salerno, A. and Angeles, J. (2007). A New Family of Two-Wheeled Mobile Robots: Modeling and Controllability. *IEEE Transactions on Robotics*, 23(1), pp.169–173. doi:https://doi.org/10.1109/tro.2006.886277.

[7] Y. Kim, S. -H. Lee and D. H. Kim, "Dynamic equations of a Wheeled Inverted Pendulum with changing its center of gravity," *2011 11th International Conference on Control, Automation and Systems*, Gyeonggi-do, Korea (South), 2011, pp. 853-854.

[8] Takei, T., Imamura, R. and Yuta, S. (2009). Baggage Transportation and Navigation by a Wheeled Inverted Pendulum Mobile Robot. *IEEE Transactions on Industrial Electronics*, 56(10), pp.3985–3994. doi:https://doi.org/10.1109/tie.2009.2027252.

[9] W. Junfeng and Z. H. Wanying (2011). Two-Wheel Self-Balancing of a Four-Wheeled Vehicle. *IEEE Control Systems*, 31(2), pp.29–37. doi:https://doi.org/10.1109/mcs.2010.939941.

[10] Pathak, K., Franch, J. and Agrawal, S.K. (2005). Velocity and position control of a wheeled inverted pendulum by partial feedback linearization. *IEEE Transactions on Robotics*, 21(3), pp.505–513. doi:https://doi.org/10.1109/tro.2004.840905.

[11] Chih-Hui Chiu (2010). The Design and Implementation of a Wheeled Inverted Pendulum Using an Adaptive Output Recurrent Cerebellar Model Articulation Controller. *IEEE Transactions on Industrial Electronics*, 57(5), pp.1814–1822. doi:https://doi.org/10.1109/tie.2009.2032203.

[12] Yau, H.-T., Wang, C.-C., Pai, N.-S. and Jang, M.-J. (2009). Robust Control Method Applied in Self-Balancing Two-Wheeled Robot. *2009 Second International Symposium on Knowledge Acquisition and Modeling*. doi:https://doi.org/10.1109/kam.2009.234.

[13] Lin, S.-C., Tsai, C.-C. and Huang, H.-C. (2009). Nonlinear adaptive sliding-mode control design for two-wheeled human transportation vehicle. *2009 IEEE International Conference on Systems, Man and Cybernetics*. doi:https://doi.org/10.1109/icsmc.2009.5346583.

[14] Junfeng Wu, Yuxin Liang and Zhe Wang (2011). A robust control method of two-wheeled self-balancing robot. *Proceedings of 2011 6th International Forum on Strategic Technology*. doi:https://doi.org/10.1109/ifost.2011.6021196.

[15] Wasif, A., Raza, D., Rasheed, W., Farooq, Z. and Ali, S.Q. (2013). Design and implementation of a two wheel self balancing robot with a two level adaptive control. *Eighth International Conference on Digital Information Management (ICDIM 2013)*. doi:https://doi.org/10.1109/icdim.2013.6694021.

[16] Pinzon-Morales, R.-D. and Hirata, Y. (2014). A portable stand-alone bi-hemispherical neuronal network model of the cerebellum for adaptive robot control. *2014 IEEE International Conference on Robotics and Biomimetics (ROBIO 2014)*. doi:https://doi.org/10.1109/robio.2014.7090487.

[17] Su, K.-H. and Chen, Y.-Y. (2010). *Balance control for two-wheeled robot via neural-fuzzy technique*. [online] IEEE Xplore. Available at: https://ieeexplore.ieee.org/stamp/stamp.jsp?tp=&arnumber=5602577&isnumber=5601973 [Accessed 11 Feb. 2023].

[18] Junfeng Wu and Shengwei Jia (2011). T-S adaptive neural network fuzzy control applied in two-wheeled self-balancing robot. *Proceedings of 2011 6th International Forum on Strategic Technology*. doi:https://doi.org/10.1109/ifost.2011.6021194.

[19] Chiu, C.-H., Lin, Y.-W. and Lin, C.-H. (2011). Real-time control of a wheeled inverted pendulum based on an intelligent model free controller. *Mechatronics*, 21(3), pp.523–533. doi:https://doi.org/10.1016/j.mechatronics.2011.01.010.

[20] Zeng, W., Wang, Q., Liu, F. and Wang, Y. (2016). Learning from adaptive neural network output feedback control of a unicycle-type mobile robot. *ISA Transactions*, 61, pp.337–347. doi:https://doi.org/10.1016/j.isatra.2016.01.005.
[21] Dai, Y., Kim, Y., Wee, S., Lee, D. and Lee, S. (2016). Symmetric caging formation for convex polygonal object transportation by multiple mobile robots based on fuzzy sliding mode control. *ISA Transactions*, 60, pp.321–332. doi:https://doi.org/10.1016/j.isatra.2015.11.017.
[22] Khooban, M., Alfi, A., & Abadi, D. (2013). Teaching–learning-based optimal interval type-2 fuzzy PID controller design: A nonholonomic wheeled mobile robots. *Robotica, 31*(7), 1059-1071. doi:10.1017/S0263574713000283
[23] Jian Huang, Zhi-Hong Guan, Matsuno, T., Fukuda, T. and Sekiyama, K. (2010). Sliding-Mode Velocity Control of Mobile-Wheeled Inverted-Pendulum Systems. *IEEE Transactions on Robotics*, 26(4), pp.750–758. doi:https://doi.org/10.1109/tro.2010.2053732.
[24] Yau, H.-T., Wang, C.-C., Pai, N.-S. and Jang, M.-J. (2009). Robust Control Method Applied in Self-Balancing Two-Wheeled Robot. *2009 Second International Symposium on Knowledge Acquisition and Modeling*. doi:https://doi.org/10.1109/kam.2009.234.
[25] Ghani, N.M.A., Yatim, N.I.M. and Azmi, N.A. (2010). *Comparative assessment for two wheels inverted pendulum mobile robot using robust control*. [online] IEEE Xplore. doi:https://doi.org/10.1109/ICCAS.2010.5669926.
[26] Junfeng Wu, Yuxin Liang and Zhe Wang (2011). A robust control method of two-wheeled self-balancing robot. *Proceedings of 2011 6th International Forum on Strategic Technology*. doi:https://doi.org/10.1109/ifost.2011.6021196.
[27] Lin, S.-C., Tsai, C.-C. and Huang, H.-C. (2009). Nonlinear adaptive sliding-mode control design for two-wheeled human transportation vehicle. *2009 IEEE International Conference on Systems, Man and Cybernetics*. doi:https://doi.org/10.1109/icsmc.2009.5346583.
[28] Dai, F., Li, F., Bai, Y., Guo, W., Zong, C. and Gao, X. (2012). Development of a coaxial self-balancing robot based on sliding mode control. *2012 IEEE International Conference on Mechatronics and Automation*. doi:https://doi.org/10.1109/icma.2012.6283528.
[29] Filipescu, A., Minzu, V., Dumitrascu, B., Filipescu, A. and Minca, E. (2011). Trajectory-tracking and discrete-time sliding-mode control of wheeled mobile robots. *2011 IEEE International Conference on Information and Automation*. doi:https://doi.org/10.1109/icinfa.2011.5948958.
[30] Yue, M., Sun, W., & Hu, P. (2011). Sliding mode robust control for two-wheeled mobile robot with lower center of gravity. *International Journal of Innovative Computing, Information and Control*, *7*(2), 637-646.
[31] Cui, M., Liu, W., Liu, H., Jiang, H. and Wang, Z. (2015). Extended state observer-based adaptive sliding mode control of differential-driving mobile robot with uncertainties. *Nonlinear Dynamics*, 83(1-2), pp.667–683. doi:https://doi.org/10.1007/s11071-015-2355-z.
[32] Wei Wang, Jianqiang Yi, Dongbin Zhao and Xiaojing Liu (2005). Double layer sliding mode control for second-order underactuated mechanical systems. *2005 IEEE/RSJ International Conference on Intelligent Robots and Systems*. doi:https://doi.org/10.1109/iros.2005.1545462.
[33] Kane, T.R. and Levinson, D.A. (1987). *Dynamics : theory and applications*. Taipei: Taipei.
[34] Kim, Y., Kim, S.H. and Kwak, Y.K. (2005). Dynamic Analysis of a Nonholonomic Two-Wheeled Inverted Pendulum Robot. *Journal of Intelligent and Robotic Systems*, 44(1), pp.25–46. doi:https://doi.org/10.1007/s10846-005-9022-4.
[35] Khalil, H.K. (2000). *Nonlinear systems*. Upper Saddle River, N.J.: Prentice Hall.